Jurnal Polimesin
Department of Mechanical Engineering
State Polytechnic of Lhokseumawe
http://e-jurnal.pnl.ac.id/polimesin

| | | | | | |
|---|---|---|---|---|---|
| e-ISSN | : 2549-1999 | No. | : 1 | Month | : February |
| p-ISSN | : 1693-5462 | Volume | : 24 | Year | : 2026 |

Processing dates: received on 2025-10-16, reviewed on 2026-1-15, accepted on 2026-01-28 and online availability on 2026-02-28

# Intelligent multi-model system for surface roughness prediction in CNC turning of multiple materials

**Rohmat Rohmat**[*], **Dianda Aryntya Firia Ferlania, Donni Frediansah Mukminin**
Department of Industrial Engineering, Muhammadiyah University, Lamongan, 62218, Indonesia
*Corresponding author: rohmat.weld@umla.ac.id

## Abstract

Surface roughness is a critical indicator of machining quality that directly affects product performance and service life. However, most existing prediction studies focus on single-material machining and rely on a single predictive model, limiting their effectiveness in real industrial environments where multiple materials are commonly processed. To address this gap, this study proposes an intelligent multimodel system for surface roughness prediction in CNC turning of multiple materials. The experimental investigation was carried out using two commonly applied steels, ST41 and S45C, with 81 machining trials performed for each material. Vibration signals were recorded using a three-axis accelerometer and combined with machining parameters consisting of feed rate, spindle speed, and depth of cut. The acquired signals were analyzed in both time and frequency domains through Fourier transformation, resulting in the extraction of eighteen vibration-related features that were normalized and used as model inputs. Three prediction techniques, namely Multiple Linear Regression, Support Vector Regression, and Artificial Neural Networks, were developed and integrated within the proposed system. System performance was evaluated using Mean Absolute Percentage Error (MAPE) and statistically analyzed through one-way ANOVA and Tukey post-hoc tests. The results demonstrate that the ANN model consistently achieved the highest prediction accuracy, with MAPE values of 2.81% for S45C, 4.72% for ST41, and 4.42% for the combined-material dataset, outperforming the Regression and SVR models. These results confirm that the proposed intelligent multimodel system provides a robust, accurate, and practical solution for vibration-based surface roughness prediction in CNC turning of multiple materials.

**Keywords:**
Intelligent multimodel, prediction, surface roughness, multiple materials, CNC turning.

## 1 Introduction

In modern manufacturing industries, machining quality is a decisive factor in determining product performance, service life, and operational reliability [1]. Among various quality indicators, surface roughness is particularly important because it directly influences mechanical strength, friction behavior, fatigue resistance, and the functional performance of machined components [2]. In CNC turning operations, inadequate control of surface roughness can lead to product defects, increased production costs, and reduced process efficiency [3]. Therefore, the development of reliable surface roughness prediction systems has become an essential objective for improving quality assurance and decision-making in CNC machining environments.

Recent research has increasingly focused on predicting surface roughness in CNC turning through the use of sensor-based monitoring and data-driven modeling techniques [4]. Vibration signals acquired using accelerometers are widely recognized as effective indicators of tool–workpiece interactions and cutting dynamics. These signals are typically processed and analyzed using statistical or machine learning models to estimate surface roughness [5][6]. Regression-based approaches have been applied due to their simplicity, while more advanced techniques such as Support Vector Regression and Artificial Neural Networks have demonstrated improved capability in capturing nonlinear machining behavior [7][8].

Despite these advances, a careful review of existing studies reveals several important limitations. Most surface roughness prediction methods are developed for single material machining, which restricts their applicability in industrial environments where multiple materials are routinely processed. In addition, many studies rely on a single prediction model, reducing robustness when machining conditions or material properties vary [9][10]. These limitations highlight the absence of an integrated multimodel system capable of delivering reliable surface roughness prediction across multiple materials in practical CNC turning applications.

To overcome these challenges, this study proposes an intelligent multimodel system for surface roughness prediction in CNC turning of multiple materials. In this study, the term “multimodel” explicitly refers to the integration and systematic comparison of three predictive models, namely Multiple Linear Regression, Support Vector Regression, and Artificial Neural Network. The proposed system is designed to evaluate and compare the predictive performance of these models under identical machining and signal conditions, thereby improving robustness and generalization. Two commonly used industrial materials, ST41 and S45C steels, are selected to represent different mechanical characteristics encountered in practical CNC turning operations. ST41 is a low carbon steel known for its good machinability and toughness, while S45C is a medium carbon steel offering higher hardness and wear resistance.

From a system implementation perspective, CNC turning experiments are conducted using spindle speed, feed rate, and depth of cut as primary machining parameters [11]. A three-axis accelerometer is employed to acquire vibration signals during the cutting process. The signals are analyzed in both time and frequency domains using Fourier transformation, and representative vibration features are extracted and normalized to serve as inputs to the prediction system [12][13]. This signal processing strategy enables the system to capture both dynamic and frequency-related characteristics of the machining process.

Within the proposed intelligent framework, the three prediction models form a unified multimodel prediction system, allowing a comprehensive evaluation of linear, machine learning, and artificial intelligence-based approaches. Prediction performance is assessed using Mean Absolute Percentage Error, and statistical significance is verified through One Way Analysis of Variance followed by Tukey post hoc tests.

The novelty of this research lies in the development of an intelligent multimodel system that combines vibration-based signal analysis, multiple predictive models, and rigorous statistical validation for surface roughness prediction in CNC turning of multiple materials. By addressing the limitations of single material and single model approaches, the proposed system offers a practical and reliable solution for industrial CNC turning applications.

## 2 Research methodology methods

Fig. 1 illustrates the structured, data-driven research framework used in this study to transform experimental machining data into reliable predictive models. The framework includes controlled data collection, comprehensive preprocessing through signal transformation, feature extraction, and normalization, and dataset partitioning for training and testing. Multiple predictive models, namely Multiple Linear Regression, Support Vector Regression, and Artificial Neural Networks, are developed to capture both linear and nonlinear relationships. Model performance is evaluated using MAPE and statistically validated through one-way ANOVA and Tukey post hoc tests, ensuring reliability, objectivity, and scientific robustness for industrial implementation.

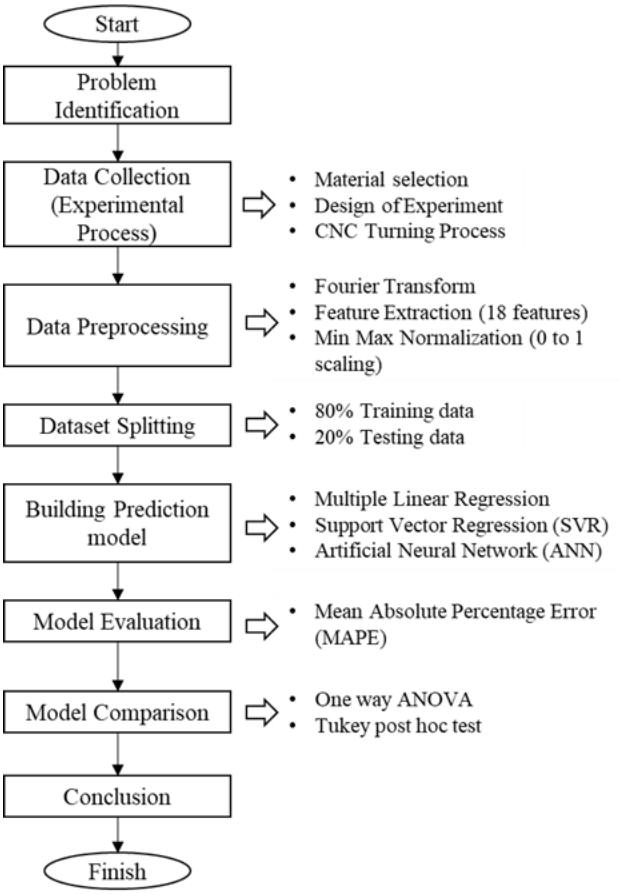

**Fig. 2.** Research flowchart

## 2.1 Data collection

### A. Material selection

This study employed two different materials. Those were ST41 and S45C. ST41 is a low-carbon structural steel commonly used in general construction and mechanical applications. It has relatively low carbon content, making it easy to machine and weld. This material is widely applied in building structures, machine components, and moderate-load parts because of its good ductility and toughness. S45C is a medium-carbon steel that provides a balance between strength and machinability. With **a** higher carbon content than ST41, S45C exhibits greater hardness, strength, and wear resistance after heat treatment. It is widely used in the manufacturing of machine parts that require higher mechanical performance, such as shafts, gears, bolts, and automotive components.

### B. Hardware

The detailed information about the hardware that was used to conduct this study can be seen in Table 1.

### C. Software

This study utilized the C# programming language to store vibration signals generated during the cutting process, which were configured and connected through DAQ204. R Studio, an open-source software, was employed to organize datasets as well as to analyze and develop prediction models. Additionally, Microsoft Excel was applied in the preprocessing stage to integrate the time-domain signals, while Minitab 17 was used to perform statistical analysis.

Table 1. Detail hardware

| No. | Item | Function |
|---|---|---|
| 1. | Personal Computer | Used for collecting data, data processing, model development, and analysis of machining signals and results. |
| 2. | CNC Turning Machine | Performs the machining process with high precision by rotating the workpiece and controlling cutting parameters automatically. |
| 3. | Machining Tool holder | Holds and secures the cutting insert or tool in place to ensure stable and accurate machining. |
| 4. | 3 axis-accelerometer | Measures vibration signals in three directions (X, Y, Z) during machining for monitoring and predictive analysis. |
| 5. | Portable roughness meter | Measures and evaluates the surface roughness of the machined workpiece directly. |
| 6. | Vernier caliper | Used to measure linear dimensions, thickness, or diameter of the workpiece with moderate precision. |
| 7. | Marker | Marks reference points or dimensions on the workpiece prior to machining or measurement. |
| 8. | Turning insert | The cutting element that removes material from the rotating workpiece during turning. |
| 9. | Vibration converter | Converts analog vibration signals from the accelerometer into digital form for computer analysis. |
| 10 | Sitting material | Provides stable support or fixture for the workpiece to minimize unwanted movement during surface roughness measurement. |

### D. Design of experiment

This study applied the design of experiment (DOE) method to establish rules for material cutting. Three cutting parameters, each with three levels, are employed based on prior studies [14][15][16]. The goal is to obtain a parameter combination that provides better results than previous works, with certain parameters adjusted to maximize outcomes. The parameters tested are spindle speed, feed rate, and depth of cut. This generates 27 experimental combinations, each repeated three times, so 81 samples of cutting each material were generated. The material length designated for cutting is 45 mm, and the detailed parameter setup is presented in Table 2. To get a combination, this study used minitab17.

Table 2. Parameter setting of experimental process

| Parameters | Levels | | |
|---|---|---|---|
| | 1 | 2 | 3 |
| Depth of cut (mm) | 0.15 | 0.2 | 0.25 |
| Feed rate (mm/rev) | 0.08 | 0.12 | 0.16 |
| Speed (rpm) | 1000 | 1400 | 1800 |

### E. Signal collection

Once the cutting process setup is completed, the operation begins and signal collection is initiated. The signals are acquired and stored using C# software. The signal acquisition processes are illustrated in Fig.2 and 3. Fig.2 shows the real-time monitoring interface developed in C#, which displays the vibration signals captured along the X, Y, and Z axes during the CNC turning process. The interface enables continuous visualization of time domain data, ensuring that the vibration response of the cutting process can be observed and recorded accurately. This real-time monitoring is essential to verify signal stability and prevent data loss during acquisition.

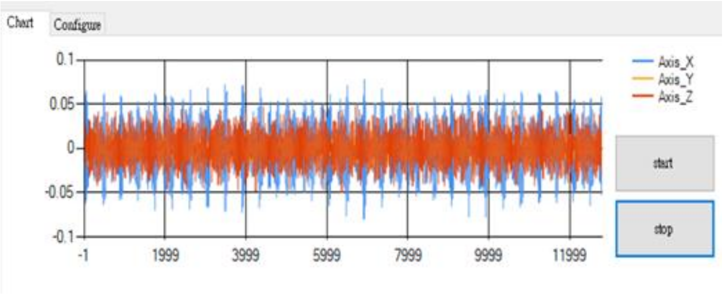

**Fig.2.** Illustrates the interface chart used for acquiring time-domain signals in C#

Fig.3 presents the configuration interface used to define the acquisition parameters prior to data collection. The sampling rate, data length, channel selection, coupling mode, input range, and sensitivity settings are configured through the DAQ204 device. These parameters determine the resolution and quality of the acquired vibration signals. Proper configuration ensures that the recorded data adequately capture the dynamic behavior of tool workpiece interactions under different machining conditions. After acquisition, the raw time domain signals are exported in CSV format and subsequently processed using Fourier transformation to convert them into the frequency domain.

Sample Rate: 12800
Data length: 12800

| | CH1 | CH2 | CH3 | CH4 |
|---|---|---|---|---|
| Coupling: | IEPE | IEPE | IEPE | AC |
| Input Range: | 1 | 1 | 1 | 1 |
| Sensitivity: | 101.20 | 101.20 | 105.70 | 1000.0 |

192.168.1.10

**Fig.3.** Illustrates the configuration interface for setting sample rates and additional parameters in C#

### F. Measuring actual surface roughness

Surface roughness was measured using a portable roughness tester. The measurement was taken at three positions on the machined surface: the front, middle, and rear. The average of these three readings was used as the representative value of the surface roughness. The detailed measurement procedure is illustrated in Fig.4.

**Fig.4.** Procedure for measuring actual surface roughness

## 2.2 Data pre-processing

### A. Conducting frequency domain analysis

At this stage, the raw time-domain signals are converted into frequency-domain signals using Fourier transformation. By utilizing R Studio and its built-in packages such as ‘periodogram’ and ‘spec,’ the frequency-domain signals can be generated efficiently, which facilitates the subsequent steps in data preprocessing.

### B. Signal extraction

Signal extraction is carried out throughout the entire process using time-domain signals. For each axis, three features are obtained from the time domain and another three from the frequency domain, resulting in a total of eighteen extracted features. These extracted signal features include the mean amplitude of the time domain (mean), root-mean-square of the time domain (RMS), peak-to-peak amplitude of the time domain, as well as frequency-domain features such as the maximum peak (max peak), the frequency corresponding to the maximum peak (max peak frequency), and the root-mean-square of the frequency domain (frequency RMS). Table 3. displays the complete output of the extracted signal features.

Table 3. The complete output of the extracted signal features

| Axis | Extraction | Factor Symbol |
|---|---|---|
| X | Mean time domain | Xmtd |
| | Peak to peak time domain | Xptpd |
| | RMS time domain | Xrmsd |
| | Maximum peak of frequency domain | Xmpfd |
| | Maximum peak corresponding frequency domain | Xmpcfd |
| | RMS frequency domain | Xrmsfd |
| Y | Mean time domain | Ymtd |
| | Peak to peak time domain | Yptpd |
| | RMS time domain | Yrmsd |
| | Maximum peak of frequency domain | Ympfd |
| | Maximum peak corresponding frequency domain | Ympcfd |
| | RMS frequency domain | Yrmsfd |
| Z | Mean time domain | Zmtd |
| | Peak to peak time domain | Zptpd |
| | RMS time domain | Zrmsd |
| | Maximum peak of frequency domain | Zmpfd |
| | Maximum peak corresponding frequency domain | Zmpcfd |
| | RMS frequency domain | Zrmsfd |

### C. Data normalization

This research employs linear regression, support vector regression, and artificial neural networks to address the problem. Prior to modeling and analysis, the signal features obtained from various processing parameters need to be normalized. To achieve this, the study applies the min–max normalization technique, which scales each set of raw signals into an interval between 0 and 1. The formulation can be seen in the equation 1.

$$g_i = \frac{f_i - \min(f)}{\max(f) - \min(f)} \tag{1}$$

Where $g_i$ and $f_i$ are the normalized value and the original $i$-th feature and *max (f)* and *min (f)* are the maximum and minimum original feature values.

### D. Determining signal factors as model inputs

At this stage, all the extracted signal features are selected to serve as inputs for multiple regression, support vector regression, and artificial neural network models.

## 2.3 Data set splitting

After preprocessing and normalization, the complete dataset was divided into two subsets to ensure objective model development and validation. A total of 80% of the data was allocated for the training phase, while the remaining 20% was reserved for testing [17][18].

The training dataset was used to build and optimize the predictive models, allowing the algorithms to learn the relationships between machining parameters, vibration features, and surface roughness values. The split was performed randomly while maintaining proportional representation of machining conditions to preserve dataset variability.

### 2.4 Building prediction model for each material and combination material

#### A. Regression model

Accordingly, this study applies Multiple Linear Regression as a predictive tool to identify how multiple factors**,** exactly all signal factors**,** collectively affect surface roughness (*Ra*). Multiple Linear Regression (MLR), is widely used to predict the value of a dependent variable based on several independent variables [19]. The model can be expressed as:

$$\hat{Y} = \beta_0 + \beta_1 X_1 + \beta_2 X_2 + \ldots\ldots + \beta_p X_p \qquad (2)$$

Where $\hat{Y}$ is the predicted response, $X_1$, $X_2$, ..$X_p$ are the predictors, $\beta_0$ is the intercept, and $\beta_1$, $\beta_2$.. $\beta_p$ are the coefficients that represent the contribution of each factor to the prediction.

The goal of multiple linear regression in prediction is to generate an accurate estimate of the response variable for new or unseen data [20]. Prediction accuracy is often evaluated using statistical metrics such as the coefficient of determination (R-Squared), which measures how well the predictors explain variation in the response, and error metrics like Mean Absolute Percentage Error (MAPE), which indicate the closeness of predictions to actual values [21].

#### B. SVR model

Support Vector Regression (SVR) is a supervised machine learning method derived from Support Vector Machines (SVM), which was originally designed for classification problems [22]. SVR adapts the principles of SVM to regression tasks, allowing it to predict continuous values. The SVR function can be expressed as:

$$f(x) = w^T x + b \qquad (3)$$

Where *w* is the weight vector, *b* is the bias (intercept), and *x* is the input vector. SVR is particularly powerful for prediction because it focuses on generalization rather than fitting all training data points exactly [23]. By using support vectors (only a subset of training points that lie outside or on the $\varepsilon$-tube), SVR achieves a sparse and robust model [24].

#### C. ANN model

An Artificial Neural Network (ANN) is a computational model inspired by the human brain, designed to recognize patterns and capture complex relationships between variables [25]. It consists of interconnected processing units called neurons, which are arranged in layers: an input layer that receives the independent variables, one or more hidden layers that transform the inputs through weighted connections and activation functions, and an output layer that produces the final prediction [26]. The strength of the connections, represented by weights, is adjusted during training to minimize prediction error. Through the use of non-linear activation functions such as sigmoid, tanh, or ReLU, ANN is capable of modeling both linear and highly non-linear data patterns [27]. The general ANN structure can be written as:

$$y = f\left(\textstyle\sum_{j-1}^{m} w_j x_j + b\right) \qquad (4)$$

Where $x_j$ represents the input variables, $w_j$ denotes the connection weights, $b$ is the bias term, $f$ (.) is the activation function that introduces nonlinearity, and $y$ corresponds to the predicted output.

The learning process in ANN involves forward propagation of data to generate predictions, followed by a loss function to calculate the error, and backpropagation to update the weights using optimization algorithms [28]. Due to its flexibility and ability to approximate complex functions, ANN is widely applied in prediction tasks across various fields.

### 2.5 Model evaluation using MAPE

Recent studies on data-driven surface roughness prediction have increasingly adopted Mean Absolute Percentage Error (MAPE) as an evaluation metric. For instance, some studies employed ANN models with vibration inputs to predict surface roughness in turning of additively-manufactured composite workpieces, achieving a MAPE indicating high predictive accuracy [5][29]. The MAPE is calculated as follows:

$$MAPE = \frac{100\%}{n} \sum_{i=1}^{n} \left| \frac{y_i - \hat{y}_i}{y_i} \right| \qquad (5)$$

Where $n$ is the total number of observations, $y_i$ is the actual surface roughness value, $\hat{y}_i$ is the predicted surface roughness value, and $|\cdot|$ is the absolute value.

### 2.6 Model comparison and result analysis using ANOVA

In this study, a one-way ANOVA will be used to determine whether there are significant differences among the three MAPE results obtained from the development of the three prediction models, as well as to identify which model performs best by considering the MAPE values [30][31]. The MAPE values were collected from five runs of each model.

## 3 Result and discussion

The analyses and results in this chapter are organized step by step, following the experimental setup and applied research methods

### 3.1 Result of actual surface roughness measurement

The machining process was conducted on a CNC turning using predetermined parameters in accordance with the design of experiments (DOE). This procedure generated surface roughness values as the model's output, while signal factors were captured as inputs for the predictive model. The resulting of surface roughness measurements is presented in the following tables. A total of 81 experimental trials were conducted for each material cutting process. In this article, only portions are presented.

Table 4. Result part of cutting S45C

| No. (Experiment) | Parameters (Depth of cut/feed rate/Speed) | Surface Roughness (Ra) ($\mu m$) |
|---|---|---|
| 1 | 0.15/0.08/1000 | 0.864 |
| 2 | 0.2/0.08/1000 | 0.913 |
| 3 | 0.25/0.08/1000 | 0.916 |
| 4 | 0.15/0.12/1000 | 1.218 |
| 5 | 0.2/0.12/1000 | 1.37 |
| 6 | 0.25/0.12/1000 | 1.732 |
| 7 | 0.15/0.16/1000 | 1.634 |
| 8 | 0.2/0.16/1000 | 1.66 |
| 9 | 0.25/0.16/1000 | 0.878 |
| 10 | 0.15/0.08/1400 | 0.862 |

Table 5. Result part of cutting ST41

| No. (Experiment) | Parameters (Depth of cut/feed rate/Speed) | Surface Roughness (Ra) ($\mu m$) |
|---|---|---|
| 1 | 0.15/0.08/1000 | 0.732 |
| 2 | 0.2/0.08/1000 | 0.703 |
| 3 | 0.25/0.08/1000 | 1.186 |
| 4 | 0.15/0.12/1000 | 1.214 |
| 5 | 0.2/0.12/1000 | 1.446 |
| 6 | 0.25/0.12/1000 | 1.426 |
| 7 | 0.15/0.16/1000 | 1.426 |
| 8 | 0.2/0.16/1000 | 0.731 |
| 9 | 0.25/0.16/1000 | 0.749 |
| 10 | 0.15/0.08/1400 | 0.763 |

### 3.2 Result of data pre-processing

The systematic steps of data preprocessing played a crucial role in preparing reliable input for predictive modeling. The conversion of raw time-domain signals into the frequency domain using Fourier transformation enables the identification of essential frequency components, thereby enhancing the interpretability of the signal data.

Subsequently, the comprehensive signal extraction process, which generated a total of eighteen features across the X, Y, and Z axes, successfully captured both time-domain and frequency-domain characteristics.

The application of min–max normalization ensured that all extracted features were transformed into a uniform scale between 0 and 1. This normalization step was essential to eliminate scale disparities among features, thus facilitating fair and effective comparisons when applying linear regression, support vector regression, and artificial neural networks.

### 3.3 Result of data pre-processing

In this article, only a portion of the normalized signal data from each cutting sample is presented. The selected input signals can be seen in the following Table 6.

Table 6. Shows result part of input model of signal factors

| Xmtd | Xptpd | Xrmsd | Xmpfd | Xmpcfd | Xrmsfd | Ymtd | Yptpd | Yrmsd | Ympfd | Ympcfd | Yrmsfd | Zmtd | Zptpd | Zrmsd | Zmpfd | Zmpcfd | Zrmsfd | Ra ($\mu m$) |
|---|---|---|---|---|---|---|---|---|---|---|---|---|---|---|---|---|---|---|
| 0.577 | 0.013 | 0.35 | 0.997 | 0.997 | 0.35 | 0.543 | 0.122 | 0.035 | 0.146 | 0.406 | 0.034 | 0.534 | 0.08 | 0.086 | 0.558 | 0.998 | 0.08 | 0.732 |
| 0.643 | 0.007 | 0.417 | 0.998 | 0.998 | 0.417 | 0.463 | 0.047 | 0.001 | 0.096 | 0.407 | 0.001 | 0.27 | 0.102 | 0.164 | 0.476 | 0.999 | 0.102 | 0.703 |
| 0.42 | 0.007 | 0.274 | 0.996 | 0.996 | 0.274 | 0.695 | 0.146 | 0.039 | 0.11 | 0.406 | 0.039 | 0.493 | 0 | 0.084 | 0.417 | 0.997 | 0 | 1.186 |
| 0.273 | 0.007 | 0.205 | 0.997 | 0.997 | 0.205 | 0.575 | 0.373 | 0.05 | 0.039 | 0.406 | 0.05 | 0.274 | 0.083 | 0.058 | 0.206 | 0.997 | 0.083 | 1.214 |
| 0.466 | 0.008 | 0.344 | 0.998 | 0.998 | 0.344 | 0.525 | 0.406 | 0.068 | 0.117 | 0.406 | 0.068 | 0.597 | 0.108 | 0.166 | 0.462 | 0.998 | 0.108 | 1.446 |
| 0.623 | 0.014 | 0.331 | 0.997 | 0.997 | 0.331 | 0.814 | 0.536 | 0.15 | 0.06 | 0.406 | 0.151 | 0.475 | 0.396 | 0.235 | 0.382 | 0.998 | 0.396 | 1.426 |
| 0.469 | 0.008 | 0.152 | 0.994 | 0.994 | 0.152 | 0.56 | 0.46 | 0.213 | 0.056 | 0.013 | 0.213 | 0.444 | 0.224 | 0.116 | 0 | 0.995 | 0.224 | 1.426 |
| 0.468 | 0.009 | 0.389 | 0.995 | 0.995 | 0.389 | 0.475 | 0.292 | 0.172 | 0.131 | 0.649 | 0.171 | 0.298 | 0.275 | 0.178 | 0.101 | 0.996 | 0.275 | 0.731 |
| 0.431 | 0.01 | 0.358 | 0.994 | 0.994 | 0.358 | 0.737 | 0.186 | 0.153 | 0.05 | 0.405 | 0.154 | 0.417 | 0.239 | 0.084 | 0.093 | 0.23 | 0.239 | 0.749 |
| 0.441 | 0.017 | 0.558 | 0.997 | 0.997 | 0.558 | 0.684 | 0.551 | 0.421 | 0.302 | 0.649 | 0.421 | 0.451 | 0.548 | 0.336 | 0.313 | 0.997 | 0.548 | 0.763 |

### 3.4 Result of prediction model

Each input dataset was divided into two subsets, consisting of 80% training data and 20% testing data. From each model, the five best MAPE samples will be selected for further processing in the subsequent stage. The data is processed using different seeds in R to obtain variations in MAPE values, which will later be compared in the subsequent test.

### 1. Regression Model

Using the multiple linear regression formula, the resulting MAPE values are as follows.

Table 7. MAPE result of regression model

| Set seed | MAPE S45C | MAPE ST41 | Mape Combination |
|---|---|---|---|
| 123 | 12.00 | 10.77 | 16.38 |
| 234 | 11.43 | 11.33 | 15.72 |
| 456 | 9.5 | 11.35 | 16.25 |
| 678 | 10.49 | 10.19 | 16.25 |
| 8910 | 10.6 | 10.42 | 16.09 |

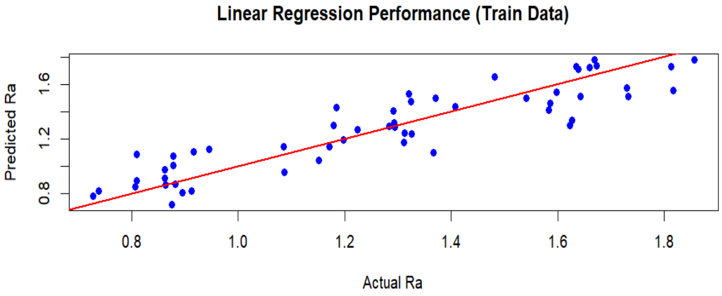

**Fig.5.** Plot actual vs prediction of S45C material

**Fig.6.** Plot actual vs prediction of ST41 material

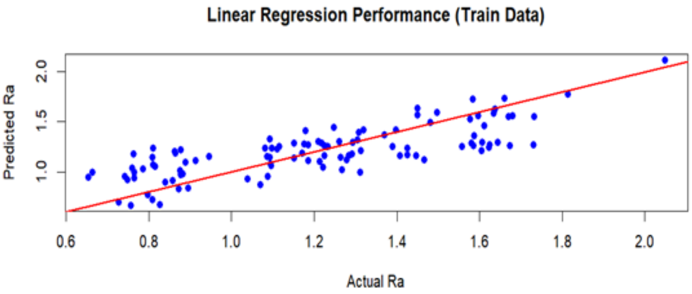

**Fig.7.** Plot actual vs prediction of combination material

From the plot above, the actual versus predicted plots indicate that the regression model provides a reasonably good fit to the training data, as most data points cluster around the ideal diagonal line, indicating close agreement between predicted and measured values. Similar visualization of regression performance has been employed in recent surface roughness prediction studies, where regression-based models demonstrate strong agreement between predicted and actual values in machining processes [32]. Minor deviations from the diagonal line are expected due to experimental noise, process variability, and intrinsic limitations of simple regression models in capturing complex machining behavior [32] . Another research also emphasizes that visual assessment through such plots should be complemented by error metrics, such as R² and MAPE, to confirm predictive accuracy [33]. Overall, the observed trends in this study align with prior findings, supporting the conclusion that the regression approach reasonably captures the relationship between inputs and measured outputs.

### 2. SVR Model

The SVR models tuned cost, gamma, and epsilon; the model can balance bias-variance trade-offs, manage tolerance to small prediction errors, and adjust sensitivity to data patterns.

Table 8. Mape result of SVR model

| Set seed | MAPE S45C | MAPE ST41 | Mape Combination |
|---|---|---|---|
| 123 | 19.23 | 20.50 | 16.57 |
| 234 | 21.87 | 18.98 | 16.53 |
| 456 | 17.37 | 20.19 | 16.58 |
| 678 | 21.42 | 15.47 | 16.55 |
| 8910 | 24.7 | 16.29 | 16.50 |

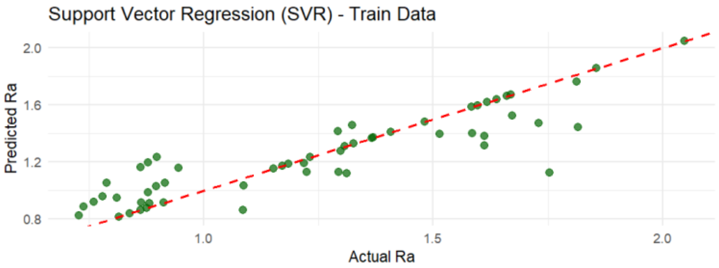

**Fig.8.** Plot actual vs prediction of S45C material

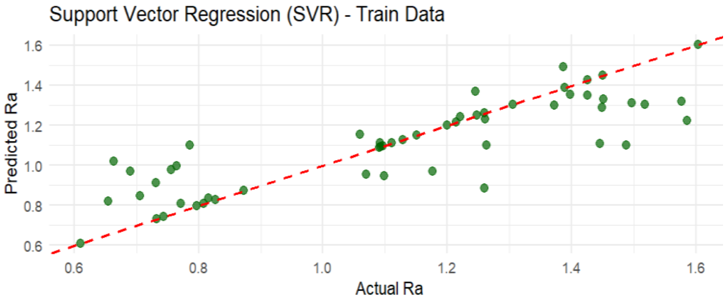

**Fig.9.** Plot actual vs prediction of ST41 material

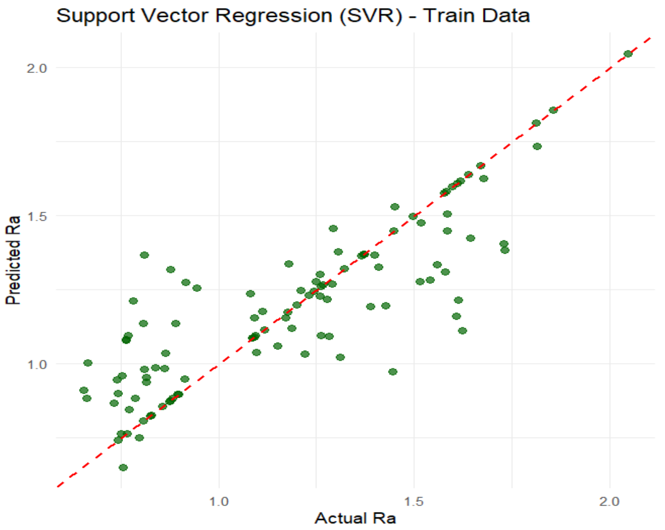

**Fig.10.** Plot actual vs prediction of combination material

From the plots above, overall, the SVR results demonstrate that the model can effectively capture the nonlinear relationship between machining parameters and surface roughness (Ra) for S45C, ST41, and combined materials, as indicated by the general alignment between predicted and actual values. The dispersion observed, particularly in the combined material dataset, is consistent with recent studies reporting that SVR performance is highly sensitive to kernel choice and hyper parameter tuning, especially when applied to limited or heterogeneous experimental data. Recent studies have shown that SVR provides reliable baseline performance in materials and mechanical property prediction, but prediction accuracy improves significantly when cost, gamma, and epsilon parameters are optimally tuned [34]. Furthermore, it has been reported that non-optimized SVR models may exhibit under fitting when dealing with complex material behavior, resulting in increased prediction error [35]. Therefore, the SVR prediction trends observed in this study are in good agreement with recent literature and confirm the suitability of SVR as a baseline regression approach.

## 3. ANN Model

The following is a complete description of the model parameters used in data processing with Artificial Neural Networks (ANN) results of model comparison.

Table 9. Parameters of ANN

| Parameter | Value / Setting | Description |
|---|---|---|
| Input Variables | 18 signal factors | Machining/measurement features from X, Y, and Z directions. |
| Output Variable | *Ra* | Target variable (surface roughness). |
| Hidden Layers | 2 | Two hidden layers for learning complex non-linear patterns. |
| Neurons per Layer | (5, 2) | First hidden layer: 5 neurons; Second hidden layer: 2 neurons. |
| Activation (Hidden) | Logistic (default in neuralnet) | Non-linear activation functions allow complex relationship modeling. |
| Activation (Output) | Linear (linear.output = TRUE) | Produces continuous numerical predictions for Ra. |
| Error Function | SSE (Sum of Squared Errors) | Objective function minimized during training. |
| Optimization Algorithm | Rprop+ (Resilient Backpropagation Plus) | Efficient weight update algorithm that adapts learning rates. |
| Max Steps | 100,000 (stepmax = 1e+05) | Maximum number of training iterations allowed. |
| Training Feedback | lifesign = "full" | Provides detailed output of training progress. |
| Data Used | training dataset | Subset of experimental/machining data used for training. |

The results are presented as follows.

Table 10. MAPE result of ANN model

| Set seed | MAPE S45C | MAPE ST41 | Mape Combination |
|---|---|---|---|
| 123 | 3.9 | 6.25 | 4.88 |
| 234 | 2.23 | 4.56 | 4.57 |
| 456 | 2.7 | 4.93 | 4.56 |
| 678 | 2.58 | 3.22 | 3.7 |
| 8910 | 2.64 | 4.66 | 4.37 |

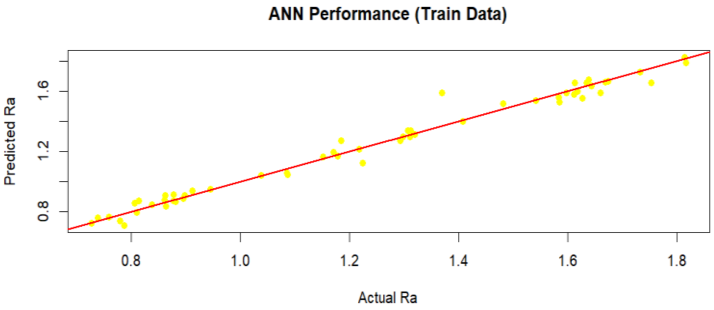

**Fig.11.** Plot actual vs prediction of S45C material

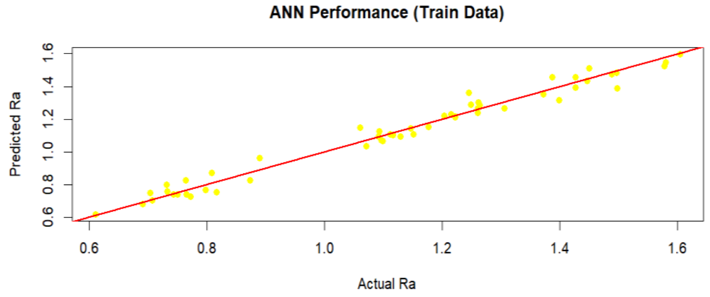

**Fig.12.** Plot actual vs prediction of ST41 material

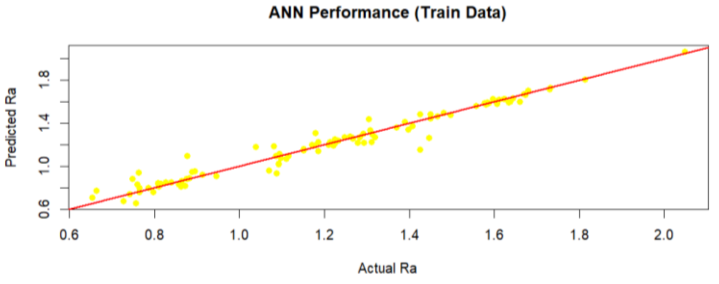

**Fig.13**. Plot actual vs prediction of combination material

Overall, the ANN model demonstrated an excellent fit to the training dataset, as evidenced by the close agreement between predicted and actual Ra values for S45C, ST41, and the combined material dataset. The near-linear distribution of data points along the regression line indicates high predictive accuracy and strong capability in capturing nonlinear relationships between machining parameters and surface roughness. Similar results have been reported in recent machining studies, where ANN-based models achieved high coefficients of determination ($R^2 > 0.95$) and low prediction errors in surface roughness prediction. Recent literature also confirms that ANN and hybrid machine learning approaches outperform conventional regression models in modeling complex machining behavior, particularly under multi-material conditions [36]. However, despite the strong training performance observed, previous studies emphasize that validation using independent test datasets is essential to prevent overfitting and ensure model robustness [37].

### 3.5 Result of model comparison

In the model comparison step, we used a one-way ANOVA analysis. Each model was compared based on the type of material using the collected MAPE values. Detailed ANOVA results can be seen in the following tables.

### 1. S45C Material

Table 11. ANOVA of S45C material

| Source | DF | Adj SS | Adj MS | F-Value | P-Value |
|---|---|---|---|---|---|
| Factor | 2 | 823.49 | 411.747 | 136.56 | 0.000 |
| Error | 12 | 36.18 | 3.015 | | |
| Total | 14 | 859.68 | | | |

The one-way ANOVA results show a statistically significant difference in MAPE values among the three models. Those are Regression, SVR, and ANN, getting a P- value of < 0.05. This indicates that the type of model has a significant effect on prediction performance for the tested material data. Further analysis, a post-hoc test, exactly Tukey test, can be performed to identify which specific models differ significantly from each other in terms of MAPE.

Table 12. Tuckey pairwise comparison of S45C material

| Factor | N | Mean | Grouping |
|---|---|---|---|
| MAPE (Regression) | 5 | 20.92 | A |
| MAPE (SVR) | 5 | 10.804 | B |
| MAPE (ANN) | 5 | 2.810 | C |

The Tukey post-hoc test results indicate that there are significant differences in prediction accuracy among the three models. The Regression model has the highest MAPE (20.92) and performs the worst, the SVR model has a moderate MAPE (10.804), and the ANN model has the lowest MAPE (2.810), indicating the best predictive performance. Since each model belongs to a different significance group (A, B, C), all differences are statistically significant, confirming that ANN outperforms SVR and Regression in predicting the material data. This result is consistent with previous studies reported that ANN significantly outperformed polynomial regression models based on ANOVA and error metrics [36]. Similarly, ANN-based models achieved higher prediction accuracy in machining applications [37] . Therefore, the present findings align with recent literature, supporting ANN as the most reliable model for surface roughness prediction.

### 2. ST41 Material

Table 13. ANOVA of ST41 material

| Source | DF | Adj SS | Adj MS | F-Value | P-Value |
|---|---|---|---|---|---|
| Factor | 2 | 461.42 | 230.710 | 103.74 | 0.000 |
| Error | 12 | 26.69 | 2.224 | | |
| Total | 14 | 488.11 | | | |

The one-way ANOVA results show a statistically significant difference in MAPE values among the three models. Those are Regression, SVR, and ANN, getting a P- value of < 0.05. This indicates that the type of model has a significant effect on prediction performance for the tested material data. Further analysis, a post-hoc test, exactly Tukey test, can be performed to identify which specific models differ significantly from each other in terms of MAPE.

Table 14. Tuckey pairwise comparison of ST41 material

| Tukey Pairwise Comparisons | | | |
|---|---|---|---|
| Factor | N | Mean | Grouping |
| MAPE (Regression) | 5 | 18.29 | A |
| MAPE (SVR) | 5 | 10.812 | B |
| MAPE (ANN) | 5 | 4.724 | C |

The Tukey post-hoc test shows that all three models differ significantly in prediction performance. Regression has the highest MAPE (18.29, Group A), SVR has a moderate MAPE (10.812, Group B), and ANN has the lowest MAPE (4.724, Group C). This confirms that ANN provides the most accurate predictions, followed by SVR, with Regression performing the worst. This outcome is consistent with recent studies. The research highlighted that ANN models significantly reduced prediction errors compared to response surface and regression approaches in hard turning operations [38]. Similarly, another study demonstrated that ANN achieved superior generalization performance validated through statistical testing [39].

### 3. Material combination

Table 15. ANOVA of material combination

| Source | DF | Adj SS | Adj MS | F-Value | P-Value |
|---|---|---|---|---|---|
| Factor | 2 | 474.514 | 237.257 | 2739.37 | 0.000 |
| Error | 12 | 1.039 | 0.087 | | |
| Total | 14 | 475.554 | | | |

The one-way ANOVA results show a statistically significant difference in MAPE values among the three models. Those are Regression, SVR, and ANN, getting a P- value of < 0.05. This indicates that the type of model has a significant effect on prediction performance for the tested material data. Further analysis, a post-hoc test, exactly Tukey test, can be performed to identify which specific models differ significantly from each other in terms of MAPE.

Table 16. Tuckey pairwise comparison of material combination

| Tukey Pairwise Comparisons | | | |
|---|---|---|---|
| Factor | N | Mean | Grouping |
| MAPE (Regression) | 5 | 16.5460 | A |
| MAPE (SVR) | 5 | 16.138 | A |
| MAPE (ANN) | 5 | 4.416 | B |

The Tukey post-hoc test indicates that the ANN model performs significantly better than both Regression and SVR models. Specifically, ANN has the lowest MAPE (4.416, Group B), while Regression (16.546) and SVR (16.138) have much higher MAPE values and are not significantly different from each other (both in Group A). These findings are consistent with recent studies. For example, ANN-based models achieved significantly lower surface roughness prediction errors than SVR and classical regression in multi-factor machining optimization [40]. Another study demonstrated that deep learning and ANN models outperform kernel-based methods such as SVR when handling nonlinear industrial datasets [41]. Collectively, these studies reinforce that ANN is more robust and reliable than traditional regression and SVR models in complex, multi-material machining environments.

## 4 Conclusion

This study developed and validated an intelligent multimodel system for vibration-based surface roughness prediction in CNC turning of multiple materials. By integrating time and frequency-domain signal processing, comprehensive feature extraction, and multimodel predictive intelligence, the proposed framework provides a robust and practical solution for machining quality prediction in industrial environments. Experimental investigations on ST41 and S45C steels, supported by a structured design of experiments, confirmed that vibration-based features effectively represent machining dynamics. 18 normalized signal features were used as model inputs for Multiple Linear Regression, Support Vector Regression, and Artificial Neural Network models developed within a unified framework. The results demonstrate that the Artificial Neural Network consistently achieves the highest prediction accuracy across all datasets, with MAPE values of 2.81% for S45C, 4.72% for ST41, and 4.42% for combined-material data. Statistical validation using one-way ANOVA and Tukey post-hoc tests confirms the significance of performance differences. Overall, the proposed system overcomes the limitations of single-material and single-model approaches and offers a scalable foundation for intelligent manufacturing and smart machining.

## 5 Acknowledgment

The authors extend their profound appreciation to the Ministry of Higher Education, Science, and Technology for the generous support and funding provided through the National Competitive Research Program, which facilitated the implementation of this research in 2025.

## References

[1] [1] P. T. B.Huang, M. M. W.Inderawati, R.Rohmat, andR.Sukwadi, "The development of an ANN surface roughness prediction system of multiple materials in CNC turning," *Int. J. Adv. Manuf. Technol.*, vol. 125, no. 3–4, pp. 1193–1211, 2023, doi: 10.1007/s00170-022-10709-y.

[2] A. T.Nguyen, V. H.Nguyen, T. T.Le, andN. T.Nguyen, "a Hybridization of Machine Learning and Nsga-Ii for Multi-Objective Optimization of Surface Roughness and Cutting Force in Aisi 4340 Alloy Steel Turning," *J. Mach. Eng.*, vol. 23, no. 1, pp. 133–153, 2023, doi: 10.36897/jme/160172.

[3] J.Chen, J.Lin, M.Zhang, andQ.Lin, "Predicting Surface Roughness in Turning Complex-Structured Workpieces Using Vibration-Signal-Based Gaussian Process Regression," *Sensors*, vol. 24, no. 7, 2024, doi: 10.3390/s24072117.

[4] E.Stathatos, E.Tzimas, P.Benardos, andG. C.Vosniakos, "Convolutional Neural Networks for Raw Signal Classification in CNC Turning Process Monitoring," *Sensors*, vol. 24, no. 5, 2024, doi: 10.3390/s24051390.

[5] A.Tzotzis, P.Maropoulos, andP.Kyratsis, "A dynamic surface roughness prediction system based on machine learning for the 3D-printed carbon-fiber-reinforced-polymer ( CFRP ) turning," *J. Intell. Manuf.*, vol. 7075, 2025, doi: 10.1007/s10845-025-02602-8.

[6] X.-Steel, "Statistical Analysis of Cutting Force and Vibration in Turning," 2025.

[7] V.Ganachari, A.Ašonja, S.Shirguppikar, andR. U.Kakade, "A Sustainable Manufacturing Approach : Experimental and Machine Learning-Based Surface Roughness Modelling in PMEDM," pp. 1–15, 2026.

[8] O.Ulkir andF.Kuncan, "Experimental Study and ANN Development for Modeling Tensile and Surface Quality of Fiber-Reinforced Nylon Composites," pp. 1–23, 2025.

[9] K.Li, B.Decost, M.Greenwood, andJ.Hattrick-simpers, "OPEN A critical examination of robustness and generalizability of machine learning prediction of materials properties," pp. 1–9, 2021, doi: 10.1038/s41524-023-01012-9.

[10] E.Ayhan, S.Güner, M.Yurdakul, andY. T.İç, "Robust parameter design for EDM - based," *J. Eng. Appl. Sci.*, pp. 1–20, 2025, doi: 10.1186/s44147-025-00618-8.

[11] Y.Akiyama, M.Iwaki, Y.Komagamine, S.Minakuchi, andM.Kanazawa, "applied sciences Effect of Spindle Speed and Feed Rate on Surface Roughness and Milling Duration in the Fabrication of Milled Complete Dentures : An In Vitro Study," 2023.

[12] M.Kodrič, J.Korbar, M.Pogačar, andG.Čepon, "Development of a resource-efficient real-time vibration-based tool condition monitoring system using PVDF accelerometers," *Measurement*, vol. 251, no. February, p. 117183, 2025, doi: 10.1016/j.measurement.2025.117183.

[13] G.Apostolou *et al.*, "Novel Framework for Quality Control in Vibration Monitoring of CNC Machining," pp. 1–20, 2024.

[14] N.Jouini, J. A.Ghani, andS.Yaqoob, "Optimized Machining Parameters for High-Speed Turning Process : A Comparative Study of Dry and Cryo + MQL Techniques," pp. 1–18, 2025.

[15] C.Srivabut, S.Rawangwong, S.Hiziroglu, andC.Homkhiew, "Composites Part C : Open Access Multi-objective optimization of turning process parameters and wood sawdust contents using response surface methodology for the minimized surface roughness of recycled plastic / wood sawdust composites," *Compos. Part C Open Access*, vol. 14, no. May, p. 100477, 2024, doi: 10.1016/j.jcomc.2024.100477.

[16] A. G.Tefera, D. K.Sinha, andG.Gupta, "Experimental investigation and optimization of cutting parameters during dry turning process of copper alloy," *J. Eng. Appl. Sci.*, pp. 1–26, 2023, doi: 10.1186/s44147-023-00314-5.

[17] Y.Kikuchi *et al.*, "Machine Learning to Predict Faricimab Treatment Outcome in Neovascular Age-Related Macular Degeneration," *Ophthalmol. Sci.*, vol. 4, no. 2, p. 100385, 2023, doi: 10.1016/j.xops.2023.100385.

[18] V.Knights, O.Petrovska, J.Bunevska-talevska, andM.Prchkovska, "Machine Learning Models and Mathematical Approaches for Predictive IoT Smart Parking," 2025.

[19] R.Jafar, A.Awad, I.Hatem, K.Jafar, E.Awad, andI.Shahrour, "smart cities Multiple Linear Regression and Machine Learning for Predicting the Drinking Water Quality Index in Al-Seine Lake," pp. 2807–2827, 2023.

[20] M.Čistý, G.Doláková, andZ.Štefunková, "through Regression Analysis : Application in Slovakia," *Environ. Process.*, 2025, doi: 10.1007/s40710-025-00747-5.

[21] L. M.Cozmuta, "Heliyon The application of multiple linear regression methods to FTIR spectra of fingernails for predicting gender and age of human subjects," *Heliyon*, vol. 11, no. 4, p. e42815, 2025, doi: 10.1016/j.heliyon.2025.e42815.

[22] B.Process, "Developing a Support Vector Regression ( SVR ) Model for Prediction of Main and Lateral Bending Angles in Laser Tube," 2023.

[23] B.Bargam, A.Boudhar, C.Kinnard, H.Bouamri, andK.Nifa, “Evaluation of the support vector regression ( SVR ) and the random forest ( RF ) models accuracy for streamflow prediction under a data - scarce basin in Morocco,” *Discov. Appl. Sci.*, 2024, doi: 10.1007/s42452-024-05994-z.

[24] G.Duan, Y.Du, Y.Shang, H.Xue, andR.Zhang, “Research on Support Vector Regression Short-Time Traffic Flow Prediction Model for Secondary Roads Based on Associated Road Analysis,” 2025.

[25] G.Kim andY.Bak, “Forward and Backpropagation-Based Artificial Neural Network Modeling Method for Power Conversion System,” pp. 1–17, 2025.

[26] V.Kartal, “Prediction of monthly evapotranspiration by artificial neural network model development with Levenberg – Marquardt method in Elazig ,” *Environ. Sci. Pollut. Res.*, vol. 31, no. 14, pp. 20953–20969, 2024, doi: 10.1007/s11356-024-32464-1.

[27] H.Begi, “Comparing MLR and ANN models for school building electrical energy prediction in Osijek-Baranja County in Croatia,” vol. 12, no. March, pp. 3595–3606, 2024, doi: 10.1016/j.egyr.2024.09.039.

[28] J. B.Deb, C.Varela, F.Faysal, Y.Wang, andC.Maiti, “Deep Artificial Neural Network Modeling of the Ablation Performance of Ceramic Matrix Composites in the Hydrogen Torch Test,” 2025.

[29] P. M.Learning, “Milling Surface Roughness Prediction Based on,” no. Learning, P. M. (2023). Milling Surface Roughness Prediction Based on., 2023.

[30] K. S.Pieczarka, “Estimating Energy Consumption During Soil Cultivation Using Geophysical Scanning and Machine Learning Methods,” pp. 1–19, 2025.

[31] M. Y. T. S.Gul, “Comprehensive comparison between artificial intelligence and multiple regression : prediction of Palmerston North ’ s temperature,” no. 2025, 2024.

[32] Y. C.Lin, K.DaWu, W. C.Shih, P. K.Hsu, andJ. P.Hung, “Prediction of surface roughness based on cutting parameters and machining vibration in end milling using regression method and artificial neural network,” *Appl. Sci.*, vol. 10, no. 11, 2020, doi: 10.3390/app10113941.

[33] M.Abdullah andS.Said, “Performance Evaluation of Machine Learning Regression Models for Rainfall Prediction,” *Iran. J. Sci. Technol. Trans. Civ. Eng.*, no. 0123456789, 2024, doi: 10.1007/s40996-024-01691-4.

[34] Q. Qin, X. Wang, S. Dai, Y. Zhong, and S. Wei, “Machine learning-based prediction of mechanical properties for large bearing housing castings,” Materials, vol. 18, no. 17, Art. no. 4036, 2025, doi: 10.3390/ma18174036.

[35] L. Li, W. Sun, L. Y. Gómez-Zamorano, Z. Liu, W. Zhang, and H. Ma, “From research trend to performance prediction: Metaheuristic-driven machine learning optimization for cement pastes containing bio-based phase change materials,” Polymers, vol. 17, no. 18, Art. no. 2541, 2025, doi: 10.3390/polym17182541.

[36] M. Petković, “Modeling and prediction of surface roughness in hybrid manufacturing—milling after FDM using artificial neural networks,” Applied Sciences, vol. 14, no. 14, Art. no. 5980, 2024, doi: 10.3390/app14145980.

[37] P. Bober, K. Zgodavová, M. Čička, M. Mihaliková, and J. Brindza, “Predictive quality analytics of surface roughness in turning operation using polynomial and artificial neural network models,” Processes, vol. 12, no. 1, Art. no. 206, 2024, doi: 10.3390/pr12010206.

[38] A. Kosarac, S. Tabaković, C. Mladjenović, and M. Željković, “Next-gen manufacturing: Machine learning for surface roughness prediction in Ti-6Al-4V biocompatible alloy machining,” Journal of Manufacturing and Materials Processing, vol. 7, no. 6, Art. no. 202, 2023, doi: 10.3390/jmmp7060202.

[39] S. Mane and R. B. Patil, “Predictive modeling of surface roughness and cutting temperature using response surface methodology and artificial neural network in hard turning of AISI 52100 steel with minimal cutting fluid application,” Machines, vol. 13, no. 4, Art. no. 266, 2025, doi: 10.3390/machines13040266.

[40] M. S. El-Asfoury, M. Baraya, E. El Shrief, K. Abdelgawad, M. Sultan, and A. Abass, “AI-based prediction of ultrasonic vibration-assisted milling performance,” Sensors, vol. 24, no. 17, Art. no. 5509, 2024, doi: 10.3390/s24175509.

[41] A. E. Muñoz-Zavala, J. E. Macías-Díaz, D. Alba-Cuéllar, and J. A. Guerrero-Díaz-de-León, “A literature review on some trends in artificial neural networks for modeling and simulation with time series,” Algorithms, vol. 17, no. 2, Art. no. 76, 2024, doi: 10.3390/a17020076.